Date: September 15, 2004 COST279TD(04)032
Issue: 01

Random Waypoint Model in n-Dimensional Space

Esa Hyytiä[1] and Jorma Virtamo[2]

Networking Laboratory, Helsinki University of Technology,
P.O. Box 3000, FIN 02015 HUT, Finland

Abstract

The random waypoint model (RWP) is one of the most widely used mobility models in performance analysis of mobile wireless networks. In this paper we extend the previous work by deriving an analytical formula for the stationary distribution of a node moving according to a RWP model in n-dimensional space.

Keywords: *mobility modeling, random waypoint model, ad hoc networking*

1 Introduction

Random waypoint model (RWP) is one of the most widely used mobility models in performance analysis of wireless ad hoc networks. In the traditional RWP model in $\mathbb{R}^2$, the path of the node is defined by a sequence of random waypoints, $P_1, P_2, \ldots,$ placed randomly using a uniform distribution in some convex domain $\mathcal{D} \subset \mathbb{R}^2$. At time $t = 0$ the node is placed at some point $P_0 \in \mathcal{D}$, either randomly using, e.g., uniform distribution or at some fixed starting point. Then the node moves at constant speed v along a line towards the next waypoint P_1. Once the node reaches waypoint P_1 it takes a new heading towards the next waypoint P_2 etc. Each line segment between two waypoints is referred to as a leg and its length is denoted by ℓ. For further details and possible extensions of the model we refer to [1].

The RWP model was originally proposed in [2] and has since then been used, e.g. in capacity and connectivity studies [3, 4, 5, 6]. The knowledge of the stationary node distribution is often needed for determining a performance quantity of interest. The stationary node distribution in RWP model (in plane) has been studied, e.g., in [7, 8, 9, 10] and an explicit formula for $\mathbb{R}^2$ was derived in [1]. In this paper we extend our earlier work in [1] by deriving an analytical formula for

[1]email: esa.hyytia@iki.fi
[2]email: jorma.virtamo@hut.fi

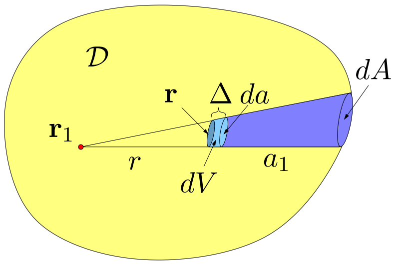

Figure 1: The integral in Eq. (3) is equal to Δ times the volume with darker shade.

stationary distribution of a node moving according to a RWP model in an n-dimensional convex set. The three-dimensional RWP process serves as an elementary model for, e.g. mobile users in an office building or a shopping center.

2 Spatial Node Distribution in $\mathbb{R}^3$

For clarity, we first consider the natural extension of RWP model to the three-dimensional space and then generalize the results to an n-dimensional space.

Let V denote the volume of the convex domain $\mathcal{D} \subset \mathbb{R}^3$, ℓ the length of an arbitrary leg and $\bar{\ell}$ the mean length of a leg. Furthermore, let $f(\mathbf{r})$ denote the pdf of the node location at $\mathbf{r}$. Similarly as in [1], we start by considering a differential volume element dV at $\mathbf{r}$ (see Fig. 1), and infer,

$$f(\mathbf{r}) = \frac{1}{\bar{\ell}} \cdot \frac{\mathrm{E}\left[\ell \cap dV\right]}{dV}, \tag{1}$$

$$\mathrm{E}\left[\ell \cap dV\right] = \frac{1}{V} \int_{\mathcal{D}} \mathrm{E}\left[\ell \cap dV | \mathbf{r}_1\right] \; d^3\mathbf{r}_1. \tag{2}$$

Let $a_1 = a_1(\mathbf{r}, \Omega)$ denote the distance from $\mathbf{r}$ to the boundary of the domain in a given direction Ω and a_2 the distance from $\mathbf{r}$ to the boundary in the opposite direction. Relying on Fig. 1 we have $dV = \Delta \cdot da$ and $da/dA = r^2/(r+a_1)^2$.

Consequently,

$$\begin{aligned}
\mathrm{E}\left[\ell \cap dV | \mathbf{r}_1\right] &= \frac{1}{V} \int_{\mathcal{D}} |\ell(\mathbf{r}_1, \mathbf{r}_2) \cap dV| \; d^3\mathbf{r}_2 \\
&= \frac{1}{3V} \Delta \cdot ((r+a_1) \cdot dA - r \cdot da) \\
&= \frac{\Delta}{3V} \cdot \left(\frac{(r+a_1)^3 - r^3}{r^2} \right) \; da = \frac{dV}{3V} \cdot \frac{(r+a_1)^3 - r^3}{r^2}.
\end{aligned} \tag{3}$$

Substituting Eqs. (2) and (3) back into Eq. (1) yields,

$$\begin{aligned}
f(\mathbf{r}) &= \frac{1}{3\bar{\ell}V^2} \int_{\mathcal{D}} \frac{(r+a_1)^3 - r^3}{r^2} \; d^3\mathbf{r}_1 \\
&= \frac{1}{3\bar{\ell}V^2} \int_{\Omega} d\Omega \int_0^{a_2} dr \; \left((r+a_1)^3 - r^3\right)
\end{aligned}$$

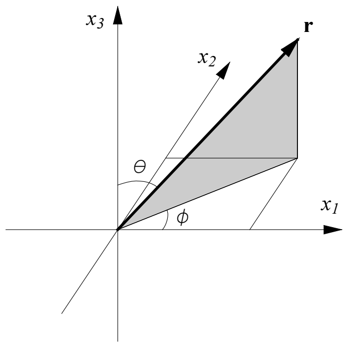

Figure 2: Spherical Coordinates.

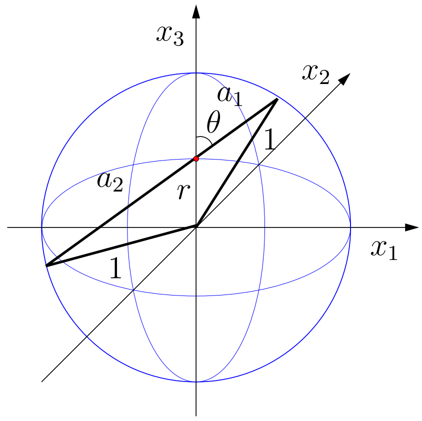

Figure 3: Due to symmetry in a unit sphere one can consider points $(0, 0, r)$ for which a_1 and a_2 are a function of r and θ.

$$= \frac{1}{12\bar{\ell}V^2} \int_\Omega d\Omega \, \left((a_1 + a_2)^4 - (a_1^4 + a_2^4)\right) .$$

More specifically, using spherical coordinates we get (see Fig. 2)

$$f(\mathbf{r}) \;\; = \frac{1}{6\bar{\ell}V^2} \int_0^\pi d\theta \, \sin\theta \int_0^\pi d\phi \; H(\mathbf{r}, \theta, \phi). \tag{4}$$

where $H(\mathbf{r}, \theta, \phi) = (a_1 + a_2)^4 - (a_1^4 + a_2^4)$.

3 Spatial Node Distribution in $\mathbb{R}^n$

The same procedure can be generalized to n dimensions. The “volume” of an n-dimensional cone is

$$V_n(h) = \frac{h \cdot A}{n},$$

where h is the height and A corresponds to the “area” of the base. Let $\mathcal{D} \subset \mathbb{R}^n$ be a convex set with volume V. Then it is easy to see that the stationary distribution of the RWP process in $\mathcal{D}$ is given by

$$f(\mathbf{r}) = \frac{1}{n\bar{\ell}V^2} \int_\mathcal{D} \frac{(r + a_1)^n - r^n}{r^{n-1}} \, d^n\mathbf{r},$$

which can be expressed as

$$f(\mathbf{r}) = \frac{1}{n(n+1)V^2\bar{\ell}} \int_\Omega d\Omega \; H(\mathbf{r}, \Omega). \tag{5}$$

where

$$H(\mathbf{r}, \Omega) = (a_1 + a_2)^{n+1} - (a_1^{n+1} + a_2^{n+1}).$$

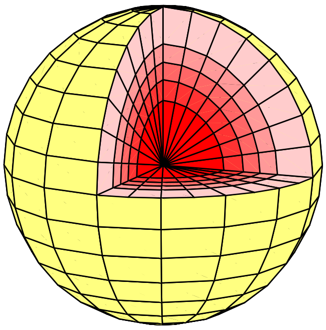

Figure 4: Stationary node distribution of the RWP process in the unit sphere. Each section represents a probability mass of 0.2.

The mean length of leg $\overline{\ell}$ is obtained from the normalization condition $\int f(\mathbf{r})\; d^n\mathbf{r} = 1$,

$$\overline{\ell} = \frac{1}{n(n+1)V^2} \int_{\mathcal{D}} d^n\mathbf{r} \int_{\Omega} d\Omega\, H(\mathbf{r},\Omega). \tag{6}$$

4 Examples

Example 1: RWP model in plane: For $n = 2$ the general expression (5) yields

$$\begin{aligned} f(\mathbf{r}) &= \frac{1}{6\overline{\ell}V^2} \int_0^{2\pi} (a_1 + a_2)^3 - (a_1^3 + a_2^3)\; d\theta \\ &= \frac{1}{\overline{\ell}V^2} \int_0^{\pi} a_1 a_2 (a_1 + a_2)\; d\theta, \end{aligned}$$

which is identical to the equation derived in [1].

Example 2: Unit sphere in $\mathbb{R}^3$: Due to the symmetry, the pdf is a function of distance $r = |\mathbf{r}|$ only and without loss of generality we can consider the point $\mathbf{r} = (0, 0, r)$. From Fig. 3 one immediately obtains that

$$\begin{aligned} a_1(r,\theta) &= \sqrt{1 - r^2 \sin^2\theta} - r\cdot\cos\theta, \\ a_2(r,\theta) &= \sqrt{1 - r^2 \sin^2\theta} + r\cdot\cos\theta. \end{aligned} \tag{7}$$

Using the 3-dimensional expression (4) we get

$$f(\mathbf{r}) = \frac{3}{16\pi\cdot\overline{\ell}} \int_0^{\pi} \overbrace{\sin\theta\cdot a_1 a_2 (2a_1^2{+}3a_1a_2{+}2a_2^2)}^{h(r,\theta)}\; d\theta.$$

Writing

$$h(r,\theta) = (1 - r^2)(7 - 3r^2 + 4r^2\cos 2\theta)\sin\theta$$

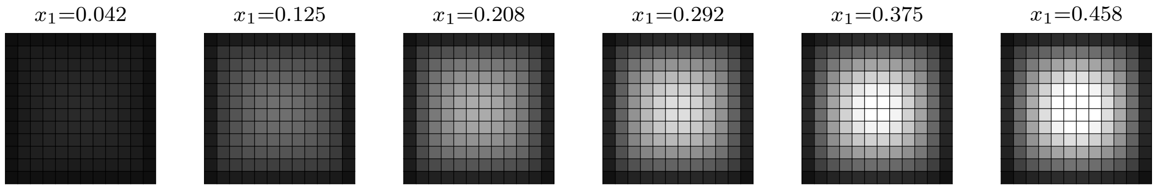

Figure 5: Pdf of the node location in the unit box at different “slices” of x_1.

and

$$h(r) = \int_0^\pi h(r, \theta)\, d\theta = \frac{2}{3}\left(21 - 34r^2 + 13r^4\right)$$

we get

$$\int_0^1 4\pi r^2 \cdot h(r)\, dr = \frac{192\pi}{35}.$$

Thus the mean length of leg $\overline{\ell}$ and the pdf of the node location at $\mathbf{r}$ are

$$\overline{\ell} = \frac{36}{35} \approx 1.029,$$
$$f(\mathbf{r}) = \frac{35}{288\pi} \cdot \left(21 - 34r^2 + 13r^4\right).$$

In the spherically symmetric case, the pdf of the random variable r, denoted by $f_d(r)$, is $f_d(r) = 4\pi r^2 f(\mathbf{r})$,

$$f_d(r) = \frac{35}{72} \cdot r^2 \left(21 - 34r^2 + 13r^4\right).$$

The cumulative pdf for the unit sphere is illustrated in Fig. 4, where each section represents a probability mass of 0.2.

Example 3: Unit box in $\mathbb{R}^3$: The next example is the unit box in 3-dimensional space. The pdf of the node location can be evaluated numerically using Eq. (4). In Fig. 5 the pdf is depicted for different values of the x_1-coordinate. Fig. 6 illustrates the marginal distribution of the node location (solid line) and the pdf of the node location in one-dimensional RWP (dashed line). It can be noted that the difference in pdfs is almost neglible.

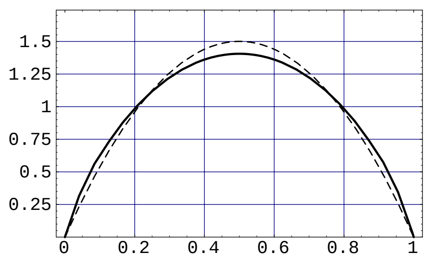

Figure 6: Marginal pdf of the node location in the unit box (solid line) compared with the pdf of the node location in 1-dimensional RWP process (dashed line).

Example 4: Unit hypersphere in $\mathbb{R}^n$: The area and volume of the n-dimensional unit hypersphere are [11]

$$A_n = \frac{2\pi^{n/2}}{\Gamma(n/2)}, \quad \text{and} \quad V_n = \frac{\pi^{n/2}}{\Gamma(n/2+1)}.$$

Again, due to the symmetry, the pdf is a function of distance $r = |\mathbf{r}|$ only and we can arbitrarily take $\mathbf{r} = (0, \ldots, 0, r)$. Eq. (7) holds still with θ being the angle between $\mathbf{r}$ and the x_n-axis. Differential surface area of the hypersphere between θ and $\theta + d\theta$ is $A_{n-1} \sin^{n-2}\theta \, d\theta$. Hence, we have

$$f(\mathbf{r}) = \frac{A_{n-1}}{n(n+1)V_n^2 \cdot \bar{\ell}} \cdot h(r),$$

where

$$\begin{aligned} h(r) &= \int_0^\pi \sin^{n-2}\theta \cdot H(r,\theta) \, d\theta, \\ H(r,\theta) &= \left((a_1+a_2)^{n+1} - (a_1^{n+1} + a_2^{n+1})\right). \end{aligned}$$

In Fig. 7 the pdf of the node location at $\mathbf{r}$, $f(\mathbf{r})$, and the pdf of the distance r from the origin, $f_d(r)$, are depicted for dimensions $n = 2, 3, 4, 5$. The maximum value of the pdf $f(r)$ attained at the center of the hypersphere increases as the dimension n increases. Furthermore, from the Fig. 7(b) it can be noted that as the dimensions increase the probability mass of the random variable r shifts towards the surface, $r = 1$. Finally, the mean length of leg given by Eq. (6) can be written for the unit hypersphere as

$$\bar{\ell}_n = \frac{A_{n-1}A_n}{n(n+1)V_n^2} \int_0^1 r^{n-1} h(r) \, dr.$$

For $n = 1, \ldots, 5$ we have explicitly

$$\begin{aligned} \bar{\ell}_1 &= 2/3 \approx 0.667, & \bar{\ell}_4 &= 16384/4725\pi \approx 1.104, \\ \bar{\ell}_2 &= 128/45\pi \approx 0.905, & \bar{\ell}_5 &= 800/693 \approx 1.154. \\ \bar{\ell}_3 &= 36/35 \approx 1.029, \end{aligned}$$

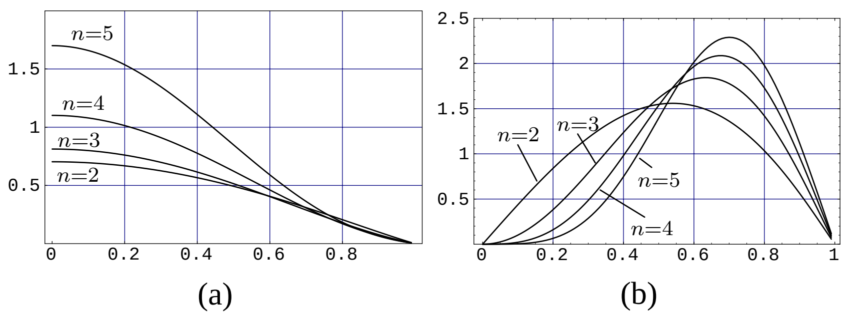

Figure 7: Pdf of the node location (left) and distance from the origin (right) in an n-dimensional unit hypersphere, $n = 2, 3, 4, 5$.

References

[1] E. Hyytiä, P. Lassila, L. Nieminen, J. Virtamo, Spatial node distribution in the random waypoint mobility model, submitted for publication (Apr. 2004).

[2] D. B. Johnson, D. A. Maltz, Dynamic source routing in ad hoc wireless networks, in: T. Imielinski, H. Korth (Eds.), Mobile Computing, Vol. 353, Kluwer Academic Publishers, 1996, pp. 153–181, chapter 5.

[3] P. Gupta, P. R. Kumar, The capacity of wireless networks, Transactions on Information Theory 46 (2).

[4] O. Dousse, P. Thiran, M. Hasler, Connectivity in ad-hoc and hybrid networks, in: Proceedings of Infocom ’02, Vol. 2, IEEE, New York, 2002, pp. 1079–1088.

[5] M. Grossglauser, D. N. C. Tse, Mobility increases the capacity of ad hoc wireless networks, IEEE/ACM Trans. Networking 10 (4).

[6] H. Koskinen, A simulation-based method for predicting connectivity in ad hoc networks, in: Proceedings of INOC 2003, Evry/Paris, France, 2003, pp. 355–360.

[7] C. Bettstetter, G. Resta, P. Santi, The node distribution of the random waypoint mobility model for wireless ad hoc networks, IEEE Transactions on Mobile Computing 2 (3) (2003) 257–269.

[8] C. Bettstetter, C. Wagner, The spatial node distribution of the random waypoint mobility model, in: Proceedings of German Workshop on Mobile Ad Hoc networks (WMAN), Ulm, Germany, 2002.

[9] W. Navidi, T. Camp, Stationary distributions for the random waypoint mobility model, IEEE Transactions on Mobile Computing 3 (1) (2004) 99–108.

[10] C. Bettstetter, H. Hartenstein, X. Pérez-Costa, Stochastic properties of the random waypoint mobility model, to appear in ACM/Kluwer Wireless Networks: Special Issue on Modeling and Analysis of Mobile Networks 10 (5).

[11] E. W. Weisstein, Hypersphere, from MathWorld – A Wolfram Web Resource. URL `http://mathworld.wolfram.com/Hypersphere.html`